Multi-species mosaicism of evolutionary origins of genomic loci harboring 59,732 human-specific regulatory sequences reflects a complex continuous speciation process of the human lineage

Gennadi V. Glinsky[1]

[1] Institute of Engineering in Medicine

University of California, San Diego

9500 Gilman Dr. MC 0435

La Jolla, CA 92093-0435, USA

Correspondence: gglinskii@ucsd.edu

Web: http://iem.ucsd.edu/people/profiles/guennadi-v-glinskii.html

Running title: Multispecies mosaicism of human-specific regulatory sequences

Key words: human-specific regulatory sequences; human-specific mutations; PtERV1 retrovirus; extinct common ancestors; non-human Great Apes; bypassing patterns of evolutionary inheritance; DNase I hypersensitive sites (DHSs); human accelerated regions; human-specific transcription factor binding sites; exaptation of ancestral regulatory DNA.

Abstract

Nearly sixty thousand genomic regions harboring various types of candidate human-specific regulatory sequences (HSRS) have been identified using high-resolution sequencing technologies and methodologically diverse comparative analyses of human and non-human primates' reference genomes. Here, the systematic analysis of evolutionary origins of 59,732 genomic loci harboring candidate HSRS has been performed to identify genomic sequences that were either inherited from extinct common ancestors (ECAs) or created de novo in human genomes after the split of human and chimpanzee lineages. Present analyses revealed thousands of HSRS that appear inherited from ECAs yet bypassed genomes of our closest evolutionary relatives, Chimpanzee and Bonobo, presumably due to the incomplete lineage sorting and/or species-specific loss or regulatory DNA. The bypassing pattern is particularly prominent for HSRS putatively associated with development and functions of human brain. Significant fractions of retrotransposon-derived loci that are transcriptionally-active in human dorsolateral prefrontal cortex are highly conserved in genomes of Gorilla, Orangutan, Gibbon, and Rhesus (1,688; 1,371; 1,148; and 1,045 loci, respectively), yet they are absent in genomes of both Chimpanzee and Bonobo. These observations were independently corroborated by common evolutionary patterns of 248 insertions sites of African ape-specific retrovirus PtERV1 (45.9%; p = 1.03E-44) intersecting genomic regions harboring 442 HSRS, which are enriched for HSRS that have been associated with human-specific (HS) changes of gene expression in cerebral organoid models of brain development. A prominent majority of genomic regions harboring HS mutations associated with HS gene expression changes during brain development is highly conserved in Chimpanzee, Bonobo, and Gorilla genomes. Among non-human primates (NHP), most significant fractions of candidate HSRS associated with HS gene expression changes in both excitatory neurons (347 loci; 67%) and radial glia (683 loci; 72%) are highly conserved in the Gorilla genome. Present analyses revealed that Modern Humans captured unique combinations of regulatory sequences, divergent subsets of which are highly conserved in distinct species of six NHP separated by 30 million years of evolution. Concurrently, this unique-to-human mosaic of genomic regulatory patterns inherited from ECAs was supplemented with 12,486 created de novo HSRS. Evidence of multispecies evolutionary origins of HSRS support the model of complex continuous speciation process during evolution of Great Apes that is not likely to occur as an instantaneous event.

Introduction

Recent advances enabled by the analyses of individual genomes of Great Apes using high-resolution sequencing technologies and methodologically diverse comparative analyses of human and non-human primates' reference genomes significantly enhanced our understanding of human-specific structural genomic variations of potential regulatory and functional significance (Locke et al., 2005; Chimpanzee Sequencing and Analysis Consortium, 2005; McLean et al., 2011; Prüfer et al., 2012; Shulha et al., 2012; Konopka et al., 2012; Scally et al., 2012; Capra et al., 2013; Marchetto et al., 2013; Marnetto et al., 2014; Prescott et al., 2015; Gittelman et al. 2015; Glinsky et al., 2015-2018; Dong et al., 2016; Sousa et al., 2017; Dennis et al., 2017; Kronenberg et al., 2018; Guffani et al., 2018). Collectively, these studies markedly expanded the compendium of candidate human-specific regulatory sequences (HSRS), which currently comprises more nearly sixty thousand genomic loci aligned to the most recent release of the human reference genome (Tables 1-4; Supplemental Tables S1-S11). This remarkable progress highlights a multitude of significant contemporary challenges, the centerpiece of which is a need to compile a comprehensive catalog of HSRS in order to identify the high-priority panel of genetic targets for stringent functional validation experiments. The selected high-priority genetic panel of human phenotypic divergence would represent the elite set of HSRS, which will be chosen based on the expectation of high-likelihood of biologically-significant species-specific effects on phenotypes that would be revealed during in-depth structural-functional explorations of their impact on development of human-specific traits.

One of essential steps toward addressing this problem is to gain insights into evolutionary origins of genomic regions harboring HSRS. In this contribution, an up-to-date catalog of 59,732 candidates human-specific regulatory loci has been assembled and their conservation patterns in genomes of five non-human Great Apes (Chimpanzee, Bonobo, Gorilla, Orangutan, and Gibbon; Tables 1-4; Supplemental Table S1-S11) have been analyzed. Systematic comparisons of genomic coordinates of HSRS and unique to African Great Apes insertions of the PtERV1 retrovirus-derived sequences were carried-out by performing comprehensive genome-wide proximity placement analyses. Diverse patterns of sequence conservation of different classes of HSRS were observed, reflecting quantitatively distinct profiles of inheritance from extinct common ancestors (ECAs) of the human lineage and each of the five species of non-human Great Apes. One of the prevalent modes of sequence conservation is represented by the bypassing pattern of evolutionary inheritance, which is exemplified by thousands of HSRS that appear inherited from ECAs yet bypassed genomes of our closest evolutionary relatives, Chimpanzee and Bonobo. The bypassing pattern of evolutionary inheritance seems particularly prominent for candidate HSRS putatively associated with development and functions of human brain.

Results

Mosaicism of evolutionary origins of genomic loci harboring various classes of human-specific mutations

Recent experiments identified 24,151 genomic regions harboring various classes of human-specific mutations identified based on the comparative analyses of genomes of Modern Humans and non-human Great Apes (Kronenber et al., 2018). It was of interest to analyze the sequence conservation patterns of these regions in genomes of six non-human primates (NHP), including five non-human Great Apes (Chimpanzee, Bonobo, Gorilla, Orangutan, and Gibbon) and Rhesus Macaque (Table 1). In these analyses, genomic sequences that manifested at least 95% of sequence conservations during the direct and reciprocal conversions from/to reference genomes of Modern Humans (hg38) and corresponding NHP species were considered highly-conserved. Within the context of definition of evolutionary origins of genomic regions harboring human-specific mutations, one of the main motivations was the inference that this analytical effort would identify highly-conserved DNA sequences that were inherited by the Modern Humans' lineage from ECAs.

Consistent with a model of the significant contribution of the ECA's inheritance, a majority (66%-88%) of 19,221 genomic loci harboring various classes of human-specific mutations appears highly conserved in genomes of Great Apes and Rhesus (Table 1). In contrast, only 13% of 4,910 human-specific short tandem repeats (STR) expansions' regions are conserved. Consistent with the predominantly primate's origins of regulatory regions harboring human-specific mutations, less than 5% of analyzed sequences appear highly conserved in the mouse genome (Table 1). Two classes of HSRS were mapped to large fractions of DNA sequences highly-conserved in genomes of various species of NHP: DNA loci harboring 49.6 to 80.6% of fixed human-specific deletions and 59.2 to 79.6% of human-specific short tandem repeats (STR) contractions were identified as highly-conserved genomic regions in genomes of different species of non-human Great Apes and Rhesus (Table 1).

Genomes of the ancestral evolutionary branch leading to human and African great apes show the significant increase in duplication activity (Marques-Bonet et al., 2009; Sudmant et al., 2013) and human-specific segmental duplications have been identified among the most promising candidate genetic loci contributing to the evolution of human-specific phenotypes (Fortna et al., 2004; Dennis et al., 2012; Charrier et al., 2012; Florio et al., 2015; Dennis et al., 2017; Kronenberg et al., 2018). It was of interest to analyze evolutionary origins of 7,987 duplicated genomic regions that were mapped to the most recent hg38 release of the human reference genome using whole-genome shotgun sequence detection (WSSD) algorithm (Kronenberg et al., 2018). Sequence conservation analyses of genomic loci duplicated in the human genome revealed that a vast majority of these regions (6,826 loci; 86.4%) are highly conserved in genomes of six non-human primates (Table 1; Supplemental Table S4; Figure 1). Interestingly, the largest fractions of both all regions successfully remapped from/to hg38 human reference genome (Table 1; Figure 1) and species-specific highly conserved regions (Supplemental Table S4; Figure 1) were observed in Gorilla and Chimpanzee genomes, indicating that these two species of non-human Great Apes are the similarly close to Modern Humans based on conservation patterns of genomic regions duplicated in the human genome. Present observations clearly demonstrate the species-specific mosaicism of evolutionary origins of genomic regions duplicated in the genome of Modern Humans (Table 1; Figure 1; Supplemental Table S4).

Mosaicism of evolutionary origins of genomic loci harboring human-specific mutations associated with human-specific gene expression changes in excitatory neurons and radial glia

Overall, the fractions of highly-conserved sequences harboring human-specific mutations and assigned to different NHP's species seem to reflect the consensus evolutionary order of the NHP genomes' similarity to the genome of Modern Humans. Most notable exceptions from this pattern were identified during the analyses of human-specific mutations associated with human-specific gene expression changes in excitatory neurons and radial glia (Tables 1 & 2). Among NHP species, a markedly prominent majority of genomic regions harboring human-specific mutations associated with human-specific gene expression changes during brain development in both excitatory neurons and radial glia is highly conserved only in genomes of our three closest evolutionary relatives: 50.9% and 50.3% in Chimpanzee; 39.9% and 47.5% in Bonobo; 67.1% and 72.1% in Gorilla (for excitatory neurons and radial glia, respectively). In contrast, only ~ 5% of genomic regions harboring human-specific mutations associated with human-specific gene expression changes detected in cerebral organoids are highly-conserved in genomes of Orangutan, Gibbon, and Rhesus. Among non-human Great Apes, most significant fractions of candidate HSRS associated with human-specific gene expression changes in both excitatory neurons (347 loci; 67%) and radial glia (683 loci; 72%) are highly conserved in the Gorilla genome. For highly-conserved regions harboring HSRS associated with human-specific gene expression changes in excitatory neurons, differences in conservation profiles between genomes of Gorilla, Chimpanzee, and Bonobo were highly significant as defined by the two-tailed Fisher's exact test (p = 1.434E-07; p = 1.574E-18; p = 0.000463). For highly-conserved regions harboring HSRS associated with human-specific gene expression changes in radial glia, differences in conservation profiles between genomes of Gorilla and Chimpanzee as well as Gorilla and Bonobo were highly significant (p = 1.623E-22 and p = 7.369E-28, respectively). In contrast, conservation profiles of HSRS associated with human-specific gene expression changes in radial glia were similar in genomes of Chimpanzee and Bonobo (p = 0.250; Table 1). These observations suggest that the majority of highly-conserved genomic regions harboring candidate HSRS associated with human-specific differences of gene expression in both excitatory neurons and radial glia was inherited from ECAs of Modern Humans and Gorilla. This conclusion remains valid when the analyses were performed considering either only loci remapped to/from NHP's genomes to identical hg38 genomic coordinates (Table 2; Figures 2-3; Supplemental Table S4) or only genomic loci uniquely mapped to genomes of only single species of non-human Great Apes (Figure 3). Notably, differences in conservation profiles of genomic loci harboring HSRS associated with human-specific gene expression changes in radial glia appear particularly prominent (Table 2; Figures 2-3; Supplemental Table S5). Consistent with the ECA's inheritance model, from 85.3% to 95.1% of HSRS-harboring regions that are highly-conserved in the genomes of Chimpanzee and Bonobo are highly-conserved in the Gorilla genome as well. In contrast, only from 59.0% to 59.3% and from 62.7% to 65.1% of

HSRS-harboring regions that are highly-conserved in the Gorilla genome remain highly-conserved in the genomes of Bonobo and Chimpanzee, respectively.

Insertion sites of the African Great Ape-specific retrovirus PtERV1 and significant fractions of distinct classes HSRS share common genomic coordinates

Structurally distinct mutations within genomic regions harboring HSRS that independently emerged on the Modern Humans lineage and distinct species of non-human Great Apes are of particular interest because they might indicate the functional divergence between species of these independently-targeted regulatory regions. In this context, it was of interest to determine whether genomic regions harboring HSRS intersect genomic coordinates of insertion sites of the African Great Ape-specific retrovirus PtERV1. Significantly, no PtERV1 insertions were detected in genomes of Modern Humans and Orangutan yet the PtERV1 retrovirus appears integrated at 540 loci in genomes of Gorilla, Chimpanzee, and Bonobo during millions years of evolution (Kronenberg et al., 2018). Analysis of evolutionary patterns of insertions of African ape-specific retrovirus PtERV1 revealed that, without exception, all distinct classes of HSRS analyzed in this study intersect within 10 Kb windows of orthologous genomic regions targeted by PtERV1 in genomes of Gorilla, Chimpanzee, and Bonobo, albeit with different degrees of frequencies and significance (Tables 3-4). Interestingly, genomic coordinates of PtERV1 insertions in the Gorilla genome appear to overlap more frequently genomic regions harboring HSRS (Table 4).

Genome-wide analysis of gene expression changes in human-chimpanzee cerebral organoids revealed that human-specific duplications, in contrast to other types of human-specific structural variations, are associated with up-regulated genes in human radial glial and excitatory neurons (Kronenberg et al., 2018). These observations are highly consistent with previous studies demonstrating that defined human-specific segmental duplications of *SRGAP2* and *ARHGAP11B* genes drive phenotypic differences in cortical development between humans and chimpanzee (Dennis et al., 2012; Charrier et al., 2012; Florio et al., 2015). Proximity placement enrichment analysis of 7,897 duplication regions in human genome and PtERV1 insertion sites (Supplemental Table S6) identified 71 PtERV1 loci intersecting 87 duplication regions and revealed significantly more frequent co-localization of Chimpanzee-specific PtERV1 insertions compared to Gorillaspecific insertions (24.2% versus 10.7%, respectively; p = 0.0076; 2-tailed Fisher's exact test). Overall, these analyses identified 248 PtERV1 loci (45.9%; p = 1.03E-44; hypergeometric distribution test) intersecting human genomic regions harboring 442 candidate HSRS (Tables 3-4), which are significantly enriched (p = 0.0018) for regions of fixed human-specific mutations that have been associated with human-specific changes of gene expression in cerebral organoids' models of brain development (Kronenberg et al., 2018). This set of genomic regions with overlapping coordinates of PtERV1 integration sites and loci harboring human-specific mutations of potential functional significance may represent an attractive functional validation panel of elite candidate regulatory sequences likely contributing to phenotypic divergence of Modern Humans and our closest evolutionary relatives.

Mosaicism of evolutionary origins of candidate human-specific regulatory loci defined based on the mapping failure to both Chimpanzee and Bonobo reference genomes

One of the approaches to the identification of candidate HSRS is based on their absence in the genomes of our closest evolutionary relatives, Chimpanzee and Bonobo. Present analyses demonstrate that large fractions of genomic regions harboring candidate HSRS are highly-conserved in genomes of our more distant evolutionary relatives, Gorilla, Orangutan, Gibbon, and Rhesus (Tables 1-2). These observations suggest that candidate human-specific regulatory loci which were defined based on the mapping failures to both Chimpanzee and Bonobo genomes may originate on DNA sequences highly-conserved in genomes of other NHP species. To test the validity of this hypothesis, 16,730 genomic loci harboring distinct classes of HSRS were identified that failed to convert to genomes of both Chimpanzee and Bonobo using 10% sequence identity threshold (Table 5). Then highly-conserved sequences in genomes of Rhesus, Gibbon, Orangutan, and Gorilla were identified and tabulated for each category of HSRS. Consistent with the bypassing patterns of evolutionary inheritance, thousands of distinct classes of candidate HSRS that failed to map to genomes of both Chimpanzee and Bonobo are highly conserved in genomes of Gorilla, Orangutan, Gibbon, and Rhesus (Table 5). Most prominently, significant fractions of retrotransposon-derived loci that are transcriptionally-active in human dorsolateral prefrontal cortex and absent in genomes of both Chimpanzee and Bonobo are highly conserved in genomes of Gorilla, Orangutan, Gibbon, and Rhesus (1,688; 1,371; 1,148; and 1,045 loci, respectively). It has been observed that in all instances the Gorilla genome had the largest numbers of shared with Modern Humans highly-conserved sequences that failed to map to genomes of both Chimpanzee and Bonobo (Supplemental Table S7).

These observations indicate that a more stringent approach for definition of candidate HSRS which are likely to have been created de novo in the genome of Modern Humans would be to require the conversion failures of a regulatory DNA sequence to all six NHP's genomes, namely genomes of Chimpanzee, Bonobo, Gorilla, Orangutan, Gibbon, and Rhesus. Using this strategy, 12,486 candidate HSRS have been identified (Supplemental Table S8), indicating that 24.8% of all analyzed in this contribution HSRS-harboring genomic loci could be classified as created de novo candidate HSRS.

Enrichment within human-specific regulatory pathways of genes comprising expression signatures of human-specific neurodevelopmental and pluripotency transcriptional networks

It is possible that distinct types of candidate HSRS are not just unrelated elements of a random population of DNA sequences, but they might represent a coherent collection of regulatory DNA sequences assembled during evolution to facilitate execution of human-specific functions. If this hypothesis is correct, then HSRS may represent the key components of human-specific genomic regulatory pathways governing human-specific gene expression patterns observed in various phenotypic contexts associated with human-specific traits. Therefore, the validity of this hypothesis could be tested using strictly-defined by comparisons with non-human Great Apes human-specific gene expression signatures associated with development of human brain in the cerebral organoid model (Kronenberg et al., 2018) and induced pluripotency phenotypes of human versus NHP cells (Marchetto et al., 2013). Kronenberg et al. (2018) identified several hundred genes that manifest human-specific expression changes in Modern Humans versus Chimpanzee cerebral organoids' model of brain development. Significant fractions of these human-specific neurodevelopmental networks operating in both excitatory neurons and radial glia appear associated with human-specific structural variants, specifically, with human-specific insertions and deletions (Supplemental Table S9). Even larger fractions of genes comprising human-specific neurodevelopmental networks have been identified as components of the gene expression signature (GES) of the MLME cells in human preimplantation embryo: common gene sets represent 262 genes

(68.2%; p = 1.59E-93) and 481 genes (72.0%; p = 3.95E-187) for human-specific GES of excitatory neurons and radial glia, respectively (Supplemental Table S9).

It has been reported that the creation of the MLME cells in human preimplantation embryos is associated with increased expression of primate-specific retrotransposon-derived regulatory long non-coding RNAs termed human pluripotency-associated transcripts, HPATs (Glinsky et al., 2018). Most recently, the expansive networks of primate-specific and human-specific retrotransposons transcriptionally active in human dorsolateral prefrontal cortex (DLPFC) and associated coding genes have been identified (Guffani et al., 2018). Thus, it was of interest to determine what fractions of genes comprising human-specific neurodevelopmental gene expression networks in excitatory neurons and radial glia may overlap with coding genes coupled with active transcription of transposable elements in human DLPFC. Remarkably, it has been observed that common gene sets represent a vast majority of genes comprising human-specific neurodevelopmental networks: they comprise 322 genes (83.9%; p = 5.57E-84) and 561 genes (84%; p = 3.08E-146) for human-specific GES of excitatory neurons and radial glia, respectively (Supplemental Table S9). Interestingly, both *SRGAP2C* and *ARHGAP11B* genes driving divergent cortical development between humans and chimpanzee (Dennis et al., 2012; Charrier et al., 2012; Florio et al., 2015) harbor transposable elements transcriptionally active in human DLPFC (Guffani et al., 2018).

Marchetto et al. (2013) identified human-specific gene expression signature distinguishing induced pluripotent stem cells (iPSC) engineered from cells of Modern Humans and NHP species. To infer the putative regulatory association patterns of genes distinguishing human iPSC versus NHP iPSC and human-specific genomic regulatory pathways, overlap enrichment analyses of corresponding gene sets have been performed. It has been observed, that the association patterns of human-specific gene expression signatures of brain development and pluripotency phenotypes with compendiums of genes likely governed by human-specific regulatory pathways appear strikingly similar (Supplemental Tables S9 and S10). Overall, 88% of genes comprising human-specific expression signature of the induced pluripotency phenotype represent genes implicated in putative regulatory associations with human-specific genomic pathways. These observations support the hypothesis that human-specific gene expression signatures of brain development and pluripotency phenotypes are associated with a collection of HSRS assembled during evolution into human-specific genomic regulatory pathways to govern transcriptional networks in human cells.

Discussion

An impressive contemporary collection of nearly sixty thousand candidate HSRS assembled by the collective decades-long effort of many laboratories (see Introduction) lends further credence to the idea that unique to human phenotypes might result from human-specific changes to genomic regulatory sequences (King and Wilson, 1975). This study identifies multiple high-priority candidate HSRS for in depth structural-functional validation analyses, among which most prominent candidate HSRS appears associated with human-specific gene expression changes in excitatory neurons and radial glia as well as in human induced pluripotent stem cells. This high-priority set of elite genetic targets include candidate HSRS putatively regulating expression of *SERINC5*, *APOBEC3B*, and *PIWIL2* genes, high expression of which in human cells is likely to confer increased resistance to the retroviral infection and propagation of retrotransposons (Marchetto et al., 2013; Usami et al., 2015; Rosa et al., 2015). It is tempting to speculate that these changes may have been significant genetic contributors conferring the selective fitness advantage to human lineage during primate evolution.

High-confidence human-specific mutations leading to emergence of candidate HSRS should be considered as rare genomic events that unlikely to occur more than once during evolution at the same genomic locations. Therefore, observations that large fractions of genomic regions harboring distinct classes of HSRS represent DNA sequences highly-conserved in genomes of distinct NHP species should be interpreted as strong circumstantial evidence consistent with their putative regulatory functions. Collectively, the evidence presented in this contribution revealed a complex unique-to-human mosaic of regulatory DNA sequences inherited from ECAs following separation events from multiple distinct NHP species and reflecting the striking ancestral polymorphism of Modern Humans. One of the novel mechanisms that may have contributed to divergence of genomic regulatory networks of Modern Humans and non-human Great Apes is illustrated by observations that the insertions of the African Great Ape-specific retrovirus PtERV1 and distinct classes of HSRS have common genomic coordinates within orthologous genomic regions of Gorilla, Chimpanzee, Bonobo, and Modern Humans. Overall, these common patterns of species-specific mutations within overlapping genomic regions were observed for 248 PtERV1 insertions and 442 HSRS, including 21 HSRS associated with genes differentially expressed in human versus chimpanzee cerebral organoid models of brain development.

Observations reported herein support the hypothesis that the speciation process during evolution of Great Apes is not likely to occur as an instantaneous event (Patterson et al., 2006): for example, human and chimpanzee lineages could have exchanged genes following the iterative sequences of the initial lineage divergence, separation, and gathering together prior to the permanent segregation of two species. Since human, chimpanzee, and gorilla lineages may have diverged during the relatively short evolutionary time, this model might reflect the extended complex speciation process of these three closely-related Great Apes, possibly involving co-evolution of their ECAs. Incomplete lineage sorting events were intrinsic components of the genomic divergence and are likely played an important role in the lineage segregation. In agreement with this hypothesis, comparative analyses of multiple alignments of sequences of human, chimpanzee, gorilla, and orangutan genomes have demonstrated that a considerable fraction of genes in the human genome is more similar to the gorilla genome than to the chimpanzee genome (Patterson et al., 2006; Chen and Li, 2001; Yang, 2002; O'hUigin et al., 2002; Wall, 2003; Hobolth et al. 2007). Genomic regions harboring HSRS appear to follow the similar evolutionary trajectory. Observed examples of the bypassing pattern of the evolutionary inheritance highlight HSRS supporting the inference of alternative genealogies (human being most closely related to NHP other than Chimpanzee) are most likely reflect the incomplete lineage sorting events. Incomplete lineage sorting has been consistently observed in the multiple alignments of the genomes for human, chimpanzee, gorilla, and orangutan where differences in models of gene genealogies and species phylogeny were documented for up to 36% of the human autosomal genome (Chen and Li, 2001; Yang, 2002; Wall, 2003; Patterson et al. 2006; Hobolth et al., 2007; 2011; Kronenberg et al., 2018). Similar changes could result from species-specific losses of conserved ancestral loci of regulatory DNA, a mechanism that contributed to evolution of human-specific traits (McLean et al., 2011).

Conclusion

Observations reported in this contribution support the conclusion that Modern Humans captured unique combinations of human-specific regulatory loci, divergent subsets of which were created within genomic regions highly conserved in distinct species of six NHP separated by 30 million years of evolution. Concurrently, this unique-to-human mosaic of genomic regulatory pathways built on DNA sequences inherited from ECAs was supplemented with 12,486 created de novo HSRS. Collectively, present findings suggest that incremental genomic divergence of the human lineage has been continued throughout the primate's evolution concurrently with the emergence and segregation of other non-human Great Ape species. This complex continuous process of genomic divergence was gradually driving speciation of *H. sapiens*, in part, by capturing and retaining the unique mosaic of genomic signatures of ECAs.

Methods

Data source

Candidate human-specific regulatory sequences and African Apes-specific retroviral insertions

A total of 51,835 candidate HSRS and all currently known 504 insertion sites of the African Apes-specific PtERV1 retrovirus were analyzed in this study, detailed descriptions of which and corresponding references of primary original contributions are reported in the Tables 1-4 and Supplemental Tables S1-S11.

Additional Data Sources and Analytical Protocols

Solely publicly available datasets and resources were used in this contribution as well as methodological approaches and a computational pipeline validated for discovery of primate-specific gene and human-specific regulatory loci (Tay et al., 2009; Kent, 2002; Schwartz et al., 2003; Capra et al., 2013; Marnetto et al., 2014; Glinsky, 2015-2018; Guffani et al., 2018). The analysis is based on the University of California Santa Cruz (UCSC) LiftOver conversion of the coordinates of human blocks to corresponding non-human genomes using chain files of pre-computed whole-genome BLASTZ alignments with a minMatch of 0.95 and other search parameters in default setting (http://genome.ucsc.edu/cgi-bin/hgLiftOver). Extraction of BLASTZ alignments by the LiftOver algorithm for a human query generates a LiftOver output "Deleted in new", which indicates that a human sequence does not intersect with any chains in a given non-human genome. This indicates the absence of the query sequence in the subject genome and was used to infer the presence or absence of the human sequence in the non-human reference genome. Human-specific regulatory sequences were manually curated to validate their identities and genomic features using a BLAST algorithm and the latest releases of the corresponding reference genome databases for time periods between April, 2013 and September, 2018.

The significance of the differences in the expected and observed numbers of events was calculated using two-tailed Fisher's exact test. Additional placement enrichment tests were performed for individual classes of HSRS taking into account the size in bp of corresponding genomic regions. Datasets of NANOG-, POU5F1-, and CTCF-binding sites and human-specific TFBS in hESCs as well as all other classes of HSRS were reported previously (Kunarso et al., 2010; McLean et al., 2011; Prüfer et al., 2012; Shulha et al., 2012; Konopka et al., 2012; Scally et al., 2012; Capra et al., 2013; Marchetto et al., 2013; Marnetto et al., 2014; Prescott et al., 2015; Gittelman et al. 2015; Glinsky et al., 2015-2018; Dong et al., 2016; Sousa et al., 2017; Dennis et al., 2017; Kronenberg et al., 2018; Guffani et al., 2018) and are publicly available.

Data analysis

Categories of DNA sequence conservation

Identification of highly-conserved in primates (pan-primate), primate-specific, and human-specific sequences was performed as previously described (Glinsky, 2015-2018). In brief, all categories were defined by direct and reciprocal mapping using liftOver (see above). Specifically:

- Highly conserved in primates' sequences: DNA sequences that have at least 95% of bases remapped during conversion from/to human (Homo sapiens, hg38), chimp (Pan troglodytes, v5), and bonobo (Pan paniscus, v2; in specifically designated instances, Pan paniscus, v1 was utilized for comparisons). Similarly, highly-conserved sequences were defined for hg38 and genomes of Gorilla, Orangutan, Gibbon, and Rhesus.
- Primate-specific: DNA sequences that failed to map to the mouse genome (mm10).
- Human-specific: DNA sequences that failed to map at least 10% of bases from human to both chimpanzee and bonobo. All candidate HSRS identified based on the sequence alignments failures to

genomes of both chimpanzee and bonobo were subjected to more stringent additional analyses requiring the mapping failures to genomes of Gorilla, Orangutan, Gibbon, and Rhesus. These loci were considered created de novo human-specific regulatory sequences (HSRS).

Additional comparisons were performed using the same methodology and exactly as stated in the manuscript text and described in details below.

Genome-wide proximity placement analysis

Genome-wide Proximity Placement Analysis (GPPA) of distinct genomic features co-localizing with HSRS was carried out as described previously (Glinsky, 2015-2018). Briefly, as typical example of the analytical protocol, we examined the significance of overlaps between hESC active enhances and hsTFBS by first identifying all hsTFBS that overlap with any of the genomic regions tested in the ChIP-STARR-seq dataset (Barakat etl, 2018; Glinsky et al., 2018). We then calculated the relative frequency of active enhancers overlapping with hsTFBS. To assess the significance of the observed overlap of genomic coordinates, we compared the values recorded for hsTFBS with the expected frequency of active and non-active enhancers that overlap with all TFBS for NANOG (15%) and OCT4 (25%) as previously determined (Barakat et al 2018). Our analyses demonstrate that more than 95% of hsTFBS co-localized with sequences in the tested regions of the hESC genome.

Evolutionary origin and functional enrichment analyses

Evolutionary origins of HSRS were inferred from the results of the conservation patterns of 59,732 candidate human-specific regulatory DNA sequences based on the hg38 release of the human reference genome and latest available releases of genomes of six non-human primates, namely Chimpanzee, Bonobo, Gorilla, Orangutan, Gibbon, and Rhesus. The conservation analyses was carried-out using the LiftOver algorithm and Multiz Alignments of 20 mammals (17 primates) of the UCSC Genome Browser (Kent et al., 2002) on Human Dec. 2013 Assembly (GRCh38/hg38) (http://genome.ucsc.edu/cgi-bin/hgTracks?db=hg38&position=chr1%3A90820922-90821071&hgsid=441235989_eelAivpkubSY2AxzLhSXKL5ut7TN).

All DNA sequences were converted to most recent releases of the corresponding reference genome databases and were utilized consistently throughout the study to ensure the use of the most precise, accurate, and reproducible genomic DNA sequences available to date. A candidate HSRS was considered conserved if it could be aligned from/to hg38 reference genome and either one or both *Chimpanzee* or *Bonobo* genomes using defined sequence conservation thresholds of the LiftOver algorithm MinMatch function and direct and reciprocal conversions protocols. Similarly, the conservation patterns were evaluated for genomes of other NHP. LiftOver conversion of the coordinates of human blocks to non-human genomes using chain files of pre-computed whole-genome BLASTZ alignments with a specified MinMatch levels and other search parameters in default setting (http://genome.ucsc.edu/cgi-bin/hgLiftOver). Several thresholds of the LiftOver algorithm MinMatch function (minimum ratio of bases that must remap) were utilized to assess the sequences conservation and identify candidate human-specific (MinMatch of 0.1; 0.95; 0.99; and 1.00) and conserved in nonhuman primates (MinMatch of 0.95 and 1.00) regulatory sequences as previously described (Glinsky, 2015-2018; Guffani et al., 2018). The Net alignments provided by the UCSC Genome Browser were utilized to compare the sequences in the human genome (hg38) with the mouse (mm10), *Chimpanzee* (PanTro5), and latest available releases of *Bonobo*, Gorilla, *Orangutan*, *Gibbon*, and *Rhesus* genomes. A given regulatory DNA segment was defined as the highly conserved regulatory sequence when both direct and reciprocal conversions between humans' and nonhuman primates' genomes were observed using the MinMatch sequence alignment threshold of 0.95 requiring that 95% of bases must remap during the alignments of the corresponding sequences. A given regulatory DNA segment was defined as the created de novo candidate human-specific regulatory sequence when sequence alignments failed to both *Chimpanzee* and *Bonobo* genomes using the specified MinMatch sequence alignment thresholds. More stringently, these requirements were extended to include genomes of Gorilla, Orangutan, Gibbon, and Rhesus. Analyses of conservation patterns of 11,866 human-specific insertions have been performed using eleven different window sizes (Supplemental Table S6) centered at the insertion sites previously reported by Kronenberg et al. (2018). Numbers of records that successfully completed direct and reciprocal conversions from/to hg38 and genomes of non-human species (six non-human primates and mouse) using sequence identity threshold 95% are reported in the Supplemental Table S11.

The Enrichr API (January 2018 version) (Chen et al., 2013) was used to test genes linked to HSRS of interest for significant enrichment in numerous functional categories. To comply with the web interface, we considered the 1000 genes closest to the tested peaks for enrichments. In all plots, we report the “combined score” calculated by Enrichr, which is a product of the significance estimate and the magnitude of enrichment (combined score $c = log(p) * z$, where p is the Fisher’s exact test p-value and z is the z-score deviation from the expected rank). Additional functional enrichment analyses were performed with GREAT (McLean et al., 2010).

Statistical Analyses of the Publicly Available Datasets

All statistical analyses of the publicly available genomic datasets, including error rate estimates, background and technical noise measurements and filtering, feature peak calling, feature selection, assignments of genomic coordinates to the corresponding builds of the reference human genome, and data visualization, were performed exactly as reported in the original publications and associated references linked to the corresponding data visualization tracks (http://genome.ucsc.edu/). Any modifications or new elements of statistical analyses are described in the corresponding sections of the Results. Statistical significance of the Pearson correlation coefficients was determined using GraphPad Prism version 6.00 software. The significance of the differences in the numbers of events between the groups was calculated using two-sided Fisher’s exact and Chi-square test, and the significance of the overlap between the events was determined using the hypergeometric distribution test (Tavazoie et al., 1999).

Supplemental Information

Supplemental information includes Supplemental Tables S1-S6.

Author Contributions

This is a single author contribution. All elements of this work, including the conception of ideas, formulation, and development of concepts, execution of experiments, analysis of data, and writing of the paper, were performed by the author.

Acknowledgements

This work was made possible by the open public access policies of major grant funding agencies and international genomic databases and the willingness of many investigators worldwide to share their primary research data. I would like to thank my anonymous colleagues for their valuable critical contributions during the peer review process of this work.

References

Barakat TS, Halbritter F, Zhang M, Rendeiro AF, Perenthaler E, Bock C, Chambers I. 2018. Functional dissection of the enhancer repertoire in human embryonic stem cells. Cell Stem Cell. 2018; 23: 276-288.e8. doi: 10.1016/j.stem.2018.06.014. Epub 2018 Jul 19.

Capra, J.A., Erwin, G.D., McKinsey, G., Rubenstein, J.L., Pollard, K.S. 2013. Many human accelerated regions are developmental enhancers. Philos Trans R Soc Lond B Biol Sci. 368 (1632): 20130025.

Charrier C, et al. 2012. Inhibition of SRGAP2 function by its human-specific paralogs induces neoteny during spine maturation. Cell 149, 923–935. doi: 10.1016/j.cell.2012.03.034; pmid: 22559944

Chen FC, Li WH. 2001. Genomic divergences between humans and other hominoids and the effective population size of the common ancestor of humans and chimpanzees. Am J Hum Genet 68: 444-456.

Chen EY, Tan CM, Kou Y, Duan Q, Wang Z, Meirelles GV, Clark NR, Ma'ayan A. 2013. Enrichr: interactive and collaborative HTML5 gene list enrichment analysis tool. BMC Bioinformatics 14, 128. doi: 10.1186/1471-2105-14-128.

Chimpanzee Sequencing and Analysis Consortium, Initial sequence of the chimpanzee genome and comparison with the human genome. 2005. Nature 437, 69–87.

Dennis MY, et al. 2012. Evolution of human-specific neural SRGAP2 genes by incomplete segmental duplication. Cell 149, 912–922. doi: 10.1016/j.cell.2012.03.033; pmid: 22559943

Dennis MY, et al. 2017. The evolution and population diversity of human-specific segmental duplications. Nat. Ecol. Evol. 1, 0069. doi: 10.1038/s41559-016-0069; pmid: 28580430

Dong X, Wang X, Zhang F, Tian W. 2016. Genome-wide identification of regulatory sequences undergoing accelerated evolution in the human genome. Mol Biol Evol. 33: 2565-75.

Florio M, et al. 2015. Human-specific gene ARHGAP11B promotes basal progenitor amplification and neocortex expansion. Science 347, 1465–1470. doi: 10.1126/science.aaa1975; pmid: 25721503

Fortna A., et al. 2004. Lineage-specific gene duplication and loss in human and great ape evolution. PLOS Biol. 2, e207. doi: 10.1371/journal.pbio.0020207; pmid: 15252450

Gittelman RM, et al. 2015. Comprehensive identification and analysis of human accelerated regulatory DNA. Genome Res. 25: 1245–1255.

Glinsky GV. 2015. Transposable elements and DNA methylation create in embryonic stem cells human-specific regulatory sequences associated with distal enhancers and non-coding RNAs. Genome Biol Evol 7: 1432-1454.

Glinsky GV. 2016. Mechanistically distinct pathways of divergent regulatory DNA creation contribute to evolution of human-specific genomic regulatory networks driving phenotypic divergence of Homo sapiens. Genome Biol Evol 8:2774-88.

Glinsky GV. 2016. Activation of endogenous human stem cell-associated retroviruses (SCARs) and therapy-resistant phenotypes of malignant tumors. Cancer Lett 376:347-359.

Glinsky GV. 2016. Single cell genomics reveals activation signatures of endogenous SCAR's networks in aneuploid human embryos and clinically intractable malignant tumors. Cancer Lett 381:176-93.

Glinsky GV. 2017. Human-specific features of pluripotency regulatory networks link NANOG with fetal and adult brain development. BioRxiv. https://www.biorxiv.org/content/early/2017/06/19/022913; doi: https://doi.org/10.1101/022913.

Glinsky GV. 2018. Contribution of transposable elements and distal enhancers to evolution of human-specific features of interphase chromatin architecture in embryonic stem cells. Chromosome Res. 2018. 26: 61-84.

Glinsky G, Durruthy-Durruthy J, Wossidlo M, Grow EJ, Weirather JL, Au KF, Wysocka J, Sebastiano V. 2018. Single cell expression analysis of primate-specific retroviruses-derived HPAT lincRNAs in viable human blastocysts identifies embryonic cells co-expressing genetic markers of multiple lineages. Heliyon 4: e00667. doi: 10.1016/j.heliyon.2018.e00667. eCollection 2018 Jun. PMID: 30003161.

Glinsky GV, Halbritter F, Barakat TS. 2018. The functional enhancer landscape in human embryonic stem cells is dominated by pan-primate and human-specific DNA sequences. In preparation.

Guffanti G, Bartlett A, Klengel T, Klengel C, Hunter R, Glinsky G, Macciardi F. 2018. Novel bioinformatics approach identifies transcriptional profiles of lineage-specific transposable elements at distinct loci in the human dorsolateral prefrontal cortex. Mol Biol Evol. doi: 10.1093/molbev/msy143. [Epub ahead of print]

Hobolth A, Christensen OF, Mailund T, Schierup MH. 2007. Genomic relationships and speciation times of human, chimpanzee, and gorilla inferred from a coalescent hidden Markov model. PLoS Genet 3: e7. doi: 10.1371/journal.pgen.0030007.

Hobolth A, Dutheil JY, Hawks J, Schierup MH, Mailund T. 2011. Incomplete lineage sorting patterns among human, chimpanzee, and orangutan suggest recent orangutan speciation and widespread selection. Genome Res. 21: 349-356. doi: 10.1101/gr.114751.110.

Kent WJ, Sugnet CW, Furey TS, Roskin KM, Pringle TH, Zahler AM, Haussler D. 2002. The Human Genome Browser at UCSC. Genome Res 12: 996-1006.

King MC, Wilson AC. 1975. Evolution at two levels in humans and chimpanzees. Science 188: 107-116. https://doi.org/10.1126/science.1090005

Konopka G, Friedrich T, Davis-Turak J, Winden K, Oldham MC, Gao F, Chen L, Wang GZ, Luo R, Preuss TM, Geschwind DH. 2012. Human-specific transcriptional networks in the brain. Neuron **75**: 601-17.

Kronenberg ZN, et al. 2018. High-resolution comparative analysis of great ape genomes. Science 360: eaar6343.

Kunarso G, Chia NY, Jeyakani J, Hwang C, Lu X, Chan YS, Ng HH, Bourque G. 2010. Transposable elements have rewired the core regulatory network of human embryonic stem cells. Nat Genet. 42: 631-634. doi: 10.1038/ng.600. Epub 2010 Jun 6. PMID: 20526341.

Locke DP, et al. 2011. Comparative and demographic analysis of orangutan genomes. Nature 469: 529–533.

Marchetto MCN, et al. 2013. Differential LINE-1 regulation in humans and other great apes. Nature 503: 525–529.

Marnetto D, Molineris I, Grassi E, Provero P. 2014. Genome-wide identification and characterization of fixed human-specific regulatory regions. Am J Hum Genet 95: 39-48.

Marques-Bonet T, et al. 2009. A burst of segmental duplications in the genome of the African great ape ancestor. Nature 457: 877–881.

McLean, C.Y., Bristor, D., Hiller, M., Clarke, S.L., Schaar, B.T., Lowe, C.B., Wenger, A.M., Bejerano, G. 2010. GREAT improves functional interpretation of cis-regulatory regions. Nat Biotechnol 28: 495-501.

McLean CY, Reno PL, Pollen AA, Bassan AI, Capellini TD, Guenther C, Indjeian VB, Lim X, Menke DB, Schaar BT, Wenger AM, Bejerano G, Kingsley DM. 2011. Human-specific loss of regulatory DNA and the evolution of human-specific traits. Nature **471**: 216-9.

O'hUigin C, Satta Y, Takahata N, Klein J. 2002. Contribution of homoplasy and of ancestral polymorphism to the evolution of genes in anthropoid primates. Mol Biol Evol 19: 1501-1513.

Patterson N, Richter DJ, Gnerre S, Lander ES, Reich D. 2006. Genetic evidence for complex speciation of human and chimpanzees. Nature 441: 1103-1108.

Prescott SL, Srinivasan R, Marchetto MC, Grishina I, Narvaiza I, Selleri L, Gage FH, Swigut T, Wysocka J. 2015. Enhancer divergence and cis-regulatory evolution in the human and chimp neural crest. Cell 163: 68-83.

Prüfer K, Munch K, Hellmann I, Akagi K, Miller JR, Walenz B, Koren S, Sutton G, Kodira C, Winer R, Knight JR, Mullikin JC, Meader SJ, Ponting CP, Lunter G, Higashino S, Hobolth A, Dutheil J, Karakoç E, Alkan C, Sajjadian S, Catacchio CR, Ventura M, Marques-Bonet T, Eichler EE, André C, Atencia R, Mugisha L, Junhold J, Patterson N, Siebauer M, Good JM, Fischer A, Ptak SE, Lachmann M, Symer DE, Mailund T, Schierup MH, Andrés AM, Kelso J, Pääbo S. 2012. The bonobo genome compared with the chimpanzee and human genomes. Nature 486:527-531.

Rosa A, Chande A, Ziglio S, De Sanctis V, Bertorelli R, Goh SL, McCauley SM, Nowosielska A, Antonarakis SE, Luban J, Santoni FA, Pizzato M. HIV-1 2015. Nef promotes infection by excluding SERINC5 from virion incorporation. Nature 526: 212-217. doi: 10.1038/nature15399

Scally A, et al. 2012. Insights into hominid evolution from the gorilla genome sequence. Nature 483, 169–175 (2012). doi: 10.1038/nature10842; pmid: 22398555

Schwartz, S., Kent, W.J., Smit, A., Zhang, Z., Baertsch, R., Hardison, R.C., Haussler, D., and Miller, W. 2003. Human-mouse alignments with BLASTZ. Genome Res. 13, 103–107.

Shulha HP, Crisci JL, Reshetov D, Tushir JS, Cheung I, Bharadwaj R, Chou HJ, Houston IB, Peter CJ, Mitchell AC, Yao WD, Myers RH, Chen JF, Preuss TM, Rogaev EI, Jensen JD, Weng Z, Akbarian S. 2012. Human-specific histone methylation signatures at transcription start sites in prefrontal neurons. PLoS Biol **10**: e1001427.

Sousa AMM, Meyer KA, Santpere G, Gulden FO, Sestan N. 2017. Evolution of the Human Nervous System Function, Structure, and Development. Cell 170:226-247.

Sudmant PH, et al. 2013. Evolution and diversity of copy number variation in the great ape lineage. Genome Res. 23, 1373–1382.

Tavazoie, S., Hughes, J.D., Campbell, M.J., Cho, R.J., and Church, GM. 1999. Systematic determination of genetic network architecture. Nat. Genet. 22, 281-285.

Tay, S.K., Blythe, J., and Lipovich, L. 2009. Global discovery of primate-specific genes in the human genome. Proc. Natl. Acad. Sci. USA 106, 12019-12024.

Usami Y, Wu Y, Göttlinger HG. 2015. SERINC3 and SERINC5 restrict HIV-1 infectivity and are counteracted by Nef. Nature 526: 218-23. doi: 10.1038/nature15400.

Wall JD. 2003. Estimating ancestral population sizes and divergence times. Genetics 163: 395-404.

Yang ZH. 2002. Likelihood and Bayes estimation of ancestral population sizes in hominoids using data from multiple loci. Genetics 162: 1811–1823.

Figure legends

Figure 1. Mosaicism of evolutionary origins of 7,897 duplicated regions in the hg38 release of human reference genome defined by whole-genome shotgun sequence detection (WSSD).

A. A consensus model of the lineage speciation during the evolution of Great Apes. The arrows depict the hypothetical flow of genomic information inherited from extinct common ancestors (ECAs) and acquired through species-specific gain and losses. Evolutionary origins via ECA's inheritance pathways of highly-conserved sequences in genomes of Modern Humans and non-human species of Great Apes are postulated.

B. Mosaicism of evolutionary origins of 7,897 duplicated regions in the hg38 release of human reference genome defined by WSSD (Kronenberg et al., 2018). Numbers of highly-conserved regions that successfully completed direct and reciprocal conversion tests are reported for each non-human species (NHS).

C. Species-specific mosaicism of evolutionary origins of duplicated regions in the hg38 release of human reference genome defined by WSSD. Only highly-conserved sequences unique for each genome of NHS are reported.

D. Linear regression analysis of duplication regions in the hg38 release of human reference genome defined by WSSD that are highly conserved in genomes of NHS. Numbers of highly-conserved sequences and numbers of lost ancestral loci are shown for each genome of NHS.

Figure 2. Mosaicism of evolutionary origins of candidate human-specific and primate-specific regulatory loci defined by sequence conservation analyses.

A. Evolutionary patterns of inheritance, gains, and losses of 540 insertions of Africa Great Apes-specific retrovirus PtERV1.

B. Evolutionary patterns of inheritance, gains, and losses of 947 human-specific regulatory regions associated with human-specific changes of gene expression in radial glia. Only records identically remapped loci in NHP during direct and reciprocal conversions from/to hg38 are reported.

C. Evolutionary patterns of inheritance, gains, and losses of 517 human-specific regulatory regions associated with human-specific changes of gene expression in excitatory neurons. Only records identically remapped loci in NHP during direct and reciprocal conversions from/to hg38 are reported.

D. Evolutionary patterns of inheritance, gains, and losses of 4645 human-specific transposable elements (TE) loci transcriptionally active in human dorsolateral prefrontal cortex (DLPFC). Common ancestor heritage number of 2361 loci takes into account 1,045 loci highly conserved in Rhesus; 4645 loci failed conversion to PanTro5 & PanPan1 (sequence identity threshold of 10%); 18 loci completed direct & reciprocal conversions (sequence identity threshold of 95%) from/to hg38 & PanPan2; 4612 failed conversions to PanTro5; PanPna1; PanPan2 (sequence identity threshold of 10%).

Figure 3. Species-specific mosaicism of evolutionary origins of human-specific regulatory sequences associated with human-specific changes of gene expression in excitatory neurons (A, B) and radial glia (C, D).

A. Highly-conserved sequences reciprocally mapped as identical loci to the 282 regions harboring human-specific mutations associated with human-specific gene expression changes in excitatory neurons.

B. Highly-conserved species-specific sequences reciprocally mapped as identical loci to the genomic regions harboring human-specific mutations associated with human-specific gene expression changes in excitatory neurons.

C. Highly-conserved sequences reciprocally mapped as identical loci to the 525 regions harboring human-specific mutations associated with human-specific gene expression changes in radial glia.

D. Highly-conserved species-specific sequences reciprocally mapped as identical loci to the genomic regions harboring human-specific mutations associated with human-specific gene expression changes in radial glia.

Figure 4. Species-specific mosaicism of evolutionary origins of human-specific regulatory sequences encoded by transcriptionally-active transposable elements (TE) in human DPLFC.

A. Numbers of sequences highly-conserved in NHP genomes reciprocally mapped to human-specific DLPFC-expressed transposable elements.

B. Highly-conserved species-specific sequences reciprocally mapped from NHP genomes to human-specific DLPFC-expressed transposable elements.

Table 1. Mosaicism of evolutionary origins of genomic loci harboring various classes of human-specific mutations: Human-specific mutations target highly conserved sequences mapped to reference genomes of multiple species of non-human primates (95% sequence identity thresholds during both direct and reciprocal conversions).

Classification category	Human genome	Chimpanzee	Percent	Bonobo	Percent	Gorilla	Percent	Orangutan	Percent	Gibbon	Percent	Rhesus	Percent	Mouse	Percent
Fixed human-specific insertions*	11886	7138	60.05	6261	52.68	7104	59.77	3209	27.00	3268	27.49	2036	17.13	0	0.00
Fixed human-specific deletions	5891	4748	80.60	4487	76.17	4542	77.10	3569	60.58	3288	55.81	2923	49.62	96	1.63
Human-specific short tandem repeats (STR) expansions	4910	272	5.54	260	5.30	236	4.81	237	4.83	298	6.07	212	4.32	131	2.67
Human-specific short tandem repeats (STR) contractions	1464	1165	79.58	1115	76.16	1165	79.58	1031	70.42	927	63.32	867	59.22	85	5.81
Human-specific mutations associated with human-specific gene expression changes in excitatory neurons**	517	263	50.87	206	39.85	347	67.12	21	4.06	25	4.84	22	4.26	0	0.00
Human-specific mutations associated with human-specific gene expression changes in radial glia**	947	476	50.26	450	47.52	683	72.12	49	5.17	41	4.33	48	5.07	0	0.00
Duplicated regions in GRCh38 space defined by WSSD***	7897	5579	70.65	4969	62.92	5692	72.08	3895	49.32	3548	44.93	3236	40.98	597	7.56

Legend: *Results of the analyses of 10Kb regions centered at the exact sites of fixed human-specific insertions are reported; **Associated with changes in gene expression in human versus chimpanzee cerebral organoids; ***WSSD, whole-genome shotgun sequence detection;

Table 2. Mosaicism of evolutionary origins of genomic loci harboring candidate human-specific regulatory sequences associated with human-specific gene expression changes in human versus chimpanzee brain organoids. Only records remapped to the identical hg38 loci are reported.

Classification category	Human genome	NHP genomes*	Percent	Chimpanzee	Percent	Bonobo	Percent	Gorilla	Percent	Orangutan	Percent	Gibbon	Percent	Rhesus	Percent	Mouse	Percent
Human-specific mutations associated with human-specific gene expression changes in excitatory neurons**	517	283	54.74	183	64.66	143	50.53	249	87.99	9	3.18	16	5.65	14	4.95	0	0.00
Human-specific mutations associated with human-specific gene expression changes in radial glia**	947	526	55.54	326	61.98	282	53.61	472	89.73	21	3.99	24	4.56	27	5.13	0	0.00

Legend: *Mapped to highly conserved regions in genomes of non-human primates (NHP) identified based on 95% sequence identity thresholds during both direct and reciprocal conversions; **Associated with changes in gene expression in human versus chimpanzee cerebral organoids; percentage values for individual genomes of non-human species reflect fractions of all records scored in non-human primates;

Table 3. Distribution profiles of human genomic regions harboring 442 loci of distinct classes of candidate HSRS co-localizing with insertion sites of 248 PtERV1 loci in Chimpanzee, Gorilla, and Bonobo genomes.

Human-specific regulatory sequences (HSRS)	Number of loci	Intersecting PtERV1 loci	Intersecting human-specific loci	Percent	P value**
Human-specific STR contractions*	1464	4	4	0.27	
Human-specific STR expansions	4910	25	25	0.51	0.374
Fixed human-specific deletions	5891	38	37	0.63	0.118
Fixed human-specific insertions	11886	66	66	0.56	0.182
All regions of human-specific mutations	24151	133	132	0.55	0.195
Fixed human-specific regulatory regions (FHSRR)	4249	15	31	0.73	0.053
Accelerated evolution-DHS (ace-DHS)	3538	23	25	0.71	0.068
Human accelerated regions (HARs)	2741	12	11	0.40	0.597
Chimp-biased developmental enhancers	999	5	5	0.50	0.499
Human segmental duplications	218	2	2	0.92	0.176
Duplicated regions in GRCh38 space defined by WSSD	7897	71	87	1.10	0.001
Human-biased developmental enhancers	996	9	10	1.00	0.026
DHS Fixed human-specific regulatory regions (DHS-FHSRR)*	2116	4	17	0.80	0.046
Human-specific functional enhancers in	1619	10	14	0.86	0.034

hESC					
Human accelerated DHS (haDHS)*	524	1	1	0.19	1
Human-specific CTCF binding sites in hESC*	575	2	3	0.52	0.410
Human-specific OCT4 binding sites in hESC*	2328	3	4	0.17	0.495
Human-specific H3K4me3 peaks in prefrontal cortex	406	5	5	1.23	0.027
Human-specific NANOG binding sites in hESC	816	14	19	2.33	5.04E-06
hESC fixed human-specific regulatory regions (hESC-FHSRR)	1932	14	29	1.50	0.00026
Human-specific TE loci expressed in DLPFC	4627	23	47	1.02	0.0046
Human-specific gene expression in brain organoids	1466	19	21	1.43	0.00087
Radial glia	947	17	19	2.01	3.43E-05
Excitatory neurons	517	5	5	0.97	0.0576
Radial glia Down	417	13	14	3.36	7.26E-07
Radial glia Up	531	4	5	0.94	0.062
Excitatory neurons Down	227	3	3	1.32	0.055
Excitatory neurons Up	291	2	2	0.69	0.261

Total number of genomic regions harboring HSRS	59732	248	442	0.74

Legend: * the overlap of genomic coordinates of PtERV1 insertions and HSRS-harboring regions of this regulatory category is not statistically significant based on the hypergeometric distribution test; ** p values were estimated using the two-tailed Fisher's exact test compared to Human-specific STR contractions category; HSRS, human-specific regulatory sequences; WSSD, whole-genome shotgun sequence detection; underlined text denotes statistically significant categories estimated by both hypergeometric distribution test and two-tailed Fisher's exact test;

Table 4. Evolutionary patterns of Chimpanzee, Gorilla, and Bonobo PtERV1 insertions intersecting genomic regions harboring HSRS.

Taxa*	Number of PtERV1 loci	PtREV1 loci intersecting genomic regions harboring human-specific regulatory loci	Percent	P value**
gorilla only	280	111	39.64	6.41E-20
chimp,gorilla	5	3	60.00	0.033
chimp,chimp,bonobo,gorilla,gorilla	1	1	100.00	0.168
chimp,chimp,bonobo,gorilla	5	0	0.00	0.399
chimp,chimp,bonobo	150	55	36.67	2.66E-09
chimp,bonobo	17	8	47.06	0.0029
chimp only	66	21	31.82	0.0012
bonobo,chimp,gorilla	1	0	0.00	0.832
bonobo,chimp	2	1	50.00	0.279
bonobo only	13	3	23.08	0.215
All PtERV1 insertions	540	203	37.59	3.24E-31
Gorilla all PtERV1 insertions	292	115	39.38	2.62E-20
Chimpanzee all PtERV1 insertions	247	89	36.03	1.71E-13
Bonobo all PtERV1 insertions	189	60	31.75	1.94E-07

Legend: * evolutionary patterns of 540 PtERV1 loci in genomes of non-human apes were reported by Kronenberg et al. (2018); ** p values were estimated using the hypergeometric distribution test considering the number of non-overlapping 10Kb regions in the human genome (308,829); the number of analyzed regions harboring HSRS (51,835); and corresponding numbers of the PtERV1 loci; no significant differences were observed between different categories;

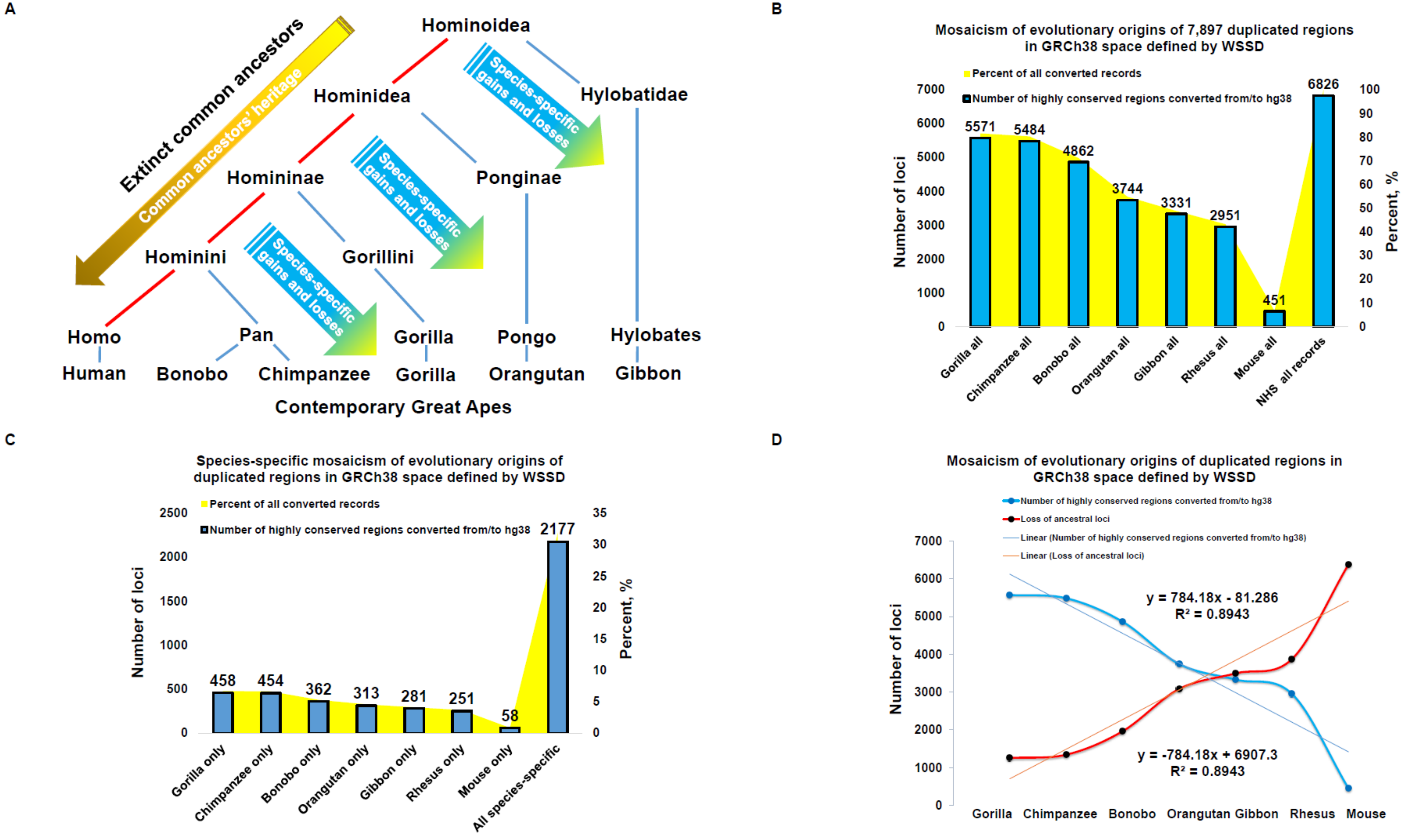
A
Extinct common ancestors
Common ancestors' heritage
Hominoidea
Hominidea
Hylobatidae
Homininae
Ponginae
Hominini
Gorillini
Species-specific gains and losses
Species-specific gains and losses
Species-specific gains and losses
Homo
Pan
Gorilla
Pongo
Hylobates
Human
Bonobo
Chimpanzee
Gorilla
Orangutan
Gibbon
Contemporary Great Apes
B
Mosaicism of evolutionary origins of 7,897 duplicated regions in GRCh38 space defined by WSSD
Percent of all converted records
Number of highly conserved regions converted from/to hg38
Number of loci
Percent, %
0
1000
2000
3000
4000
5000
6000
7000
0
10
20
30
40
50
60
70
80
90
100
5571
5484
4862
3744
3331
2951
451
6826
Gorilla all
Chimpanzee all
Bonobo all
Orangutan all
Gibbon all
Rhesus all
Mouse all
NHS all records
C
Species-specific mosaicism of evolutionary origins of duplicated regions in GRCh38 space defined by WSSD
Percent of all converted records
Number of highly conserved regions converted from/to hg38
Number of loci
Percent, %
0
500
1000
1500
2000
2500
0
5
10
15
20
25
30
35
458
454
362
313
281
251
58
2177
Gorilla only
Chimpanzee only
Bonobo only
Orangutan only
Gibbon only
Rhesus only
Mouse only
All species-specific
D
Mosaicism of evolutionary origins of duplicated regions in GRCh38 space defined by WSSD
Number of highly conserved regions converted from/to hg38
Loss of ancestral loci
Linear (Number of highly conserved regions converted from/to hg38)
Linear (Loss of ancestral loci)
Number of loci
0
1000
2000
3000
4000
5000
6000
7000
y = 784.18x - 81.286
R² = 0.8943
y = -784.18x + 6907.3
R² = 0.8943
Gorilla
Chimpanzee
Bonobo
Orangutan
Gibbon
Rhesus
Mouse

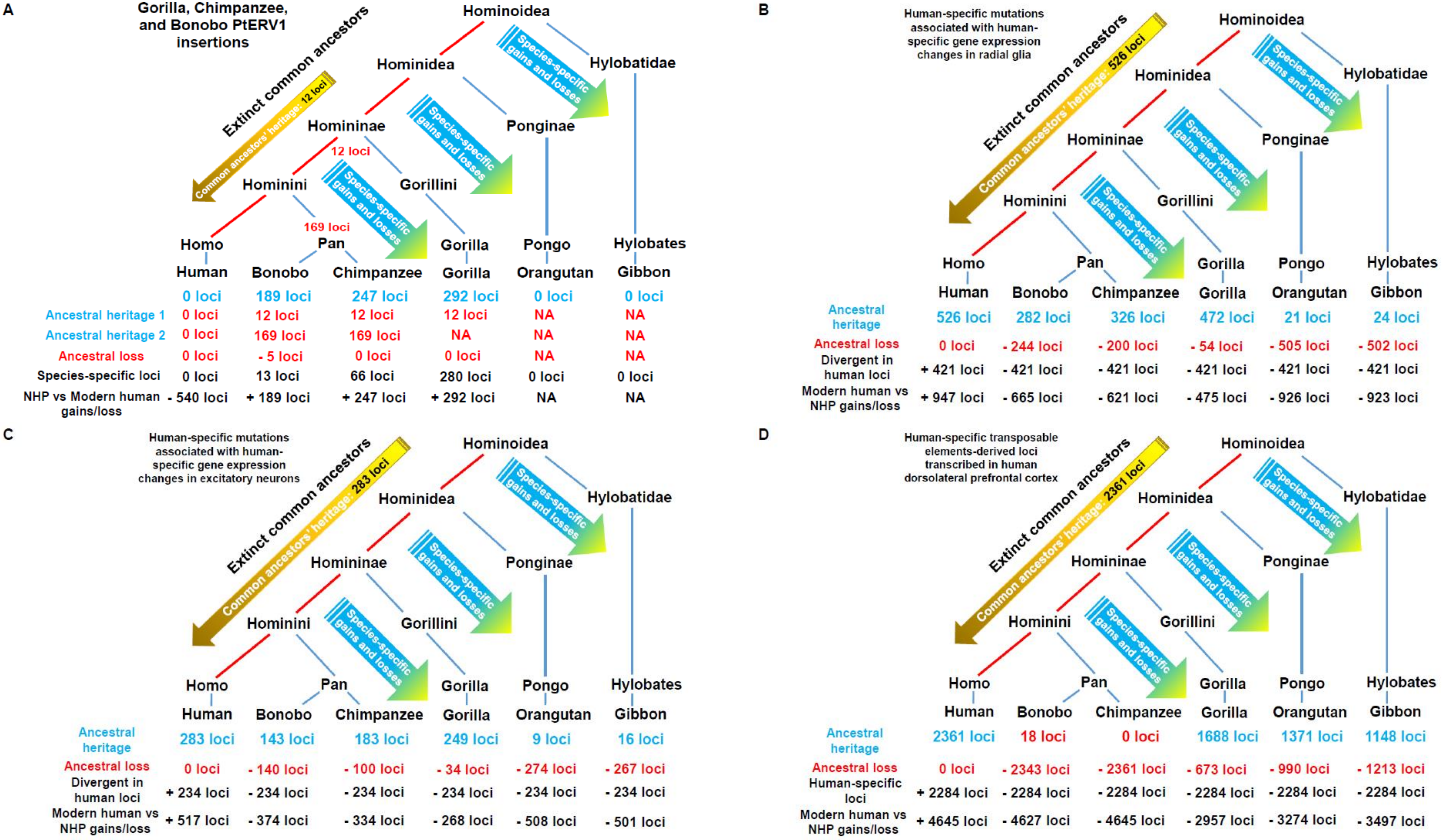
A
Gorilla, Chimpanzee, and Bonobo PtERV1 insertions
Extinct common ancestors
Common ancestors' heritage: 12 loci
Hominoidea
Hominidea
Hylobatidae
Homininae
Ponginae
12 loci
Hominini
Gorillini
169 loci
Homo
Pan
Gorilla
Pongo
Hylobates
Species-specific gains and losses
Human
Bonobo
Chimpanzee
Gorilla
Orangutan
Gibbon
B
Human-specific mutations associated with human-specific gene expression changes in radial glia
Extinct common ancestors
Common ancestors' heritage: 526 loci
C
Human-specific mutations associated with human-specific gene expression changes in excitatory neurons
Extinct common ancestors
Common ancestors' heritage: 283 loci
D
Human-specific transposable elements-derived loci transcribed in human dorsolateral prefrontal cortex
Extinct common ancestors
Common ancestors' heritage: 2361 loci

A

	Human	Bonobo	Chimpanzee	Gorilla	Orangutan	Gibbon
	0 loci	189 loci	247 loci	292 loci	0 loci	0 loci
Ancestral heritage 1	0 loci	12 loci	12 loci	12 loci	NA	NA
Ancestral heritage 2	0 loci	169 loci	169 loci	NA	NA	NA
Ancestral loss	0 loci	- 5 loci	0 loci	0 loci	NA	NA
Species-specific loci	0 loci	13 loci	66 loci	280 loci	0 loci	0 loci
NHP vs Modern human gains/loss	- 540 loci	+ 189 loci	+ 247 loci	+ 292 loci	NA	NA

B

	Human	Bonobo	Chimpanzee	Gorilla	Orangutan	Gibbon
Ancestral heritage	526 loci	282 loci	326 loci	472 loci	21 loci	24 loci
Ancestral loss	0 loci	- 244 loci	- 200 loci	- 54 loci	- 505 loci	- 502 loci
Divergent in human loci	+ 421 loci	- 421 loci	- 421 loci	- 421 loci	- 421 loci	- 421 loci
Modern human vs NHP gains/loss	+ 947 loci	- 665 loci	- 621 loci	- 475 loci	- 926 loci	- 923 loci

C

	Human	Bonobo	Chimpanzee	Gorilla	Orangutan	Gibbon
Ancestral heritage	283 loci	143 loci	183 loci	249 loci	9 loci	16 loci
Ancestral loss	0 loci	- 140 loci	- 100 loci	- 34 loci	- 274 loci	- 267 loci
Divergent in human loci	+ 234 loci	- 234 loci	- 234 loci	- 234 loci	- 234 loci	- 234 loci
Modern human vs NHP gains/loss	+ 517 loci	- 374 loci	- 334 loci	- 268 loci	- 508 loci	- 501 loci

D

	Human	Bonobo	Chimpanzee	Gorilla	Orangutan	Gibbon
Ancestral heritage	2361 loci	18 loci	0 loci	1688 loci	1371 loci	1148 loci
Ancestral loss	0 loci	- 2343 loci	- 2361 loci	- 673 loci	- 990 loci	- 1213 loci
Human-specific loci	+ 2284 loci	- 2284 loci	- 2284 loci	- 2284 loci	- 2284 loci	- 2284 loci
Modern human vs NHP gains/loss	+ 4645 loci	- 4627 loci	- 4645 loci	- 2957 loci	- 3274 loci	- 3497 loci

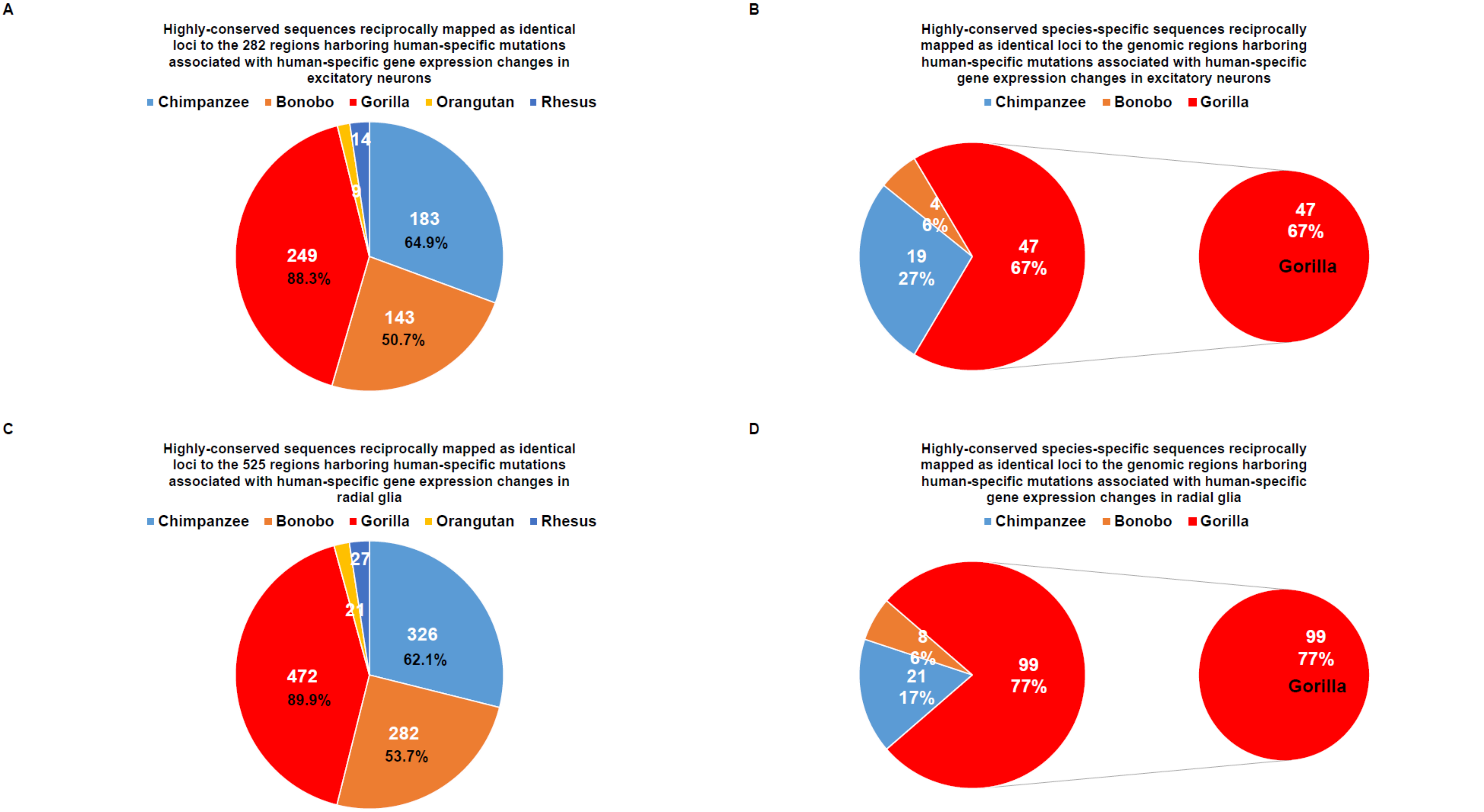

A

Highly-conserved sequences reciprocally mapped as identical loci to the 282 regions harboring human-specific mutations associated with human-specific gene expression changes in excitatory neurons

B

Highly-conserved species-specific sequences reciprocally mapped as identical loci to the genomic regions harboring human-specific mutations associated with human-specific gene expression changes in excitatory neurons

C

Highly-conserved sequences reciprocally mapped as identical loci to the 525 regions harboring human-specific mutations associated with human-specific gene expression changes in radial glia

D

Highly-conserved species-specific sequences reciprocally mapped as identical loci to the genomic regions harboring human-specific mutations associated with human-specific gene expression changes in radial glia

A

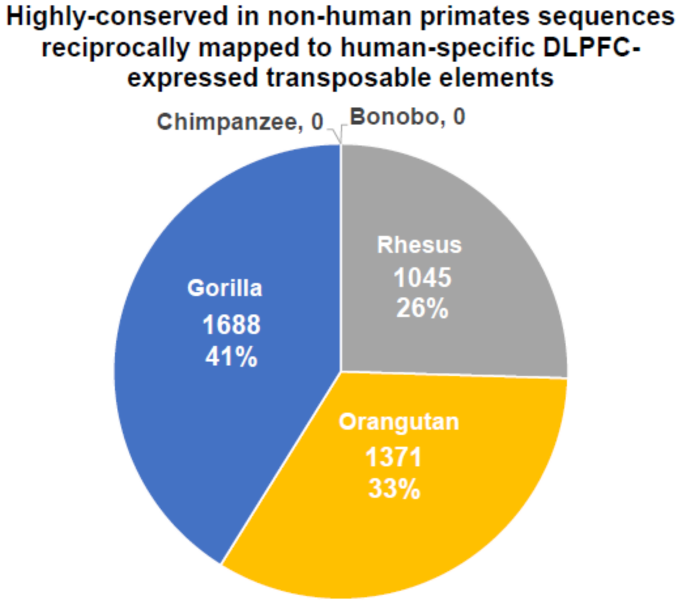

DLPFC, dorsolateral prefrontal cortex

B

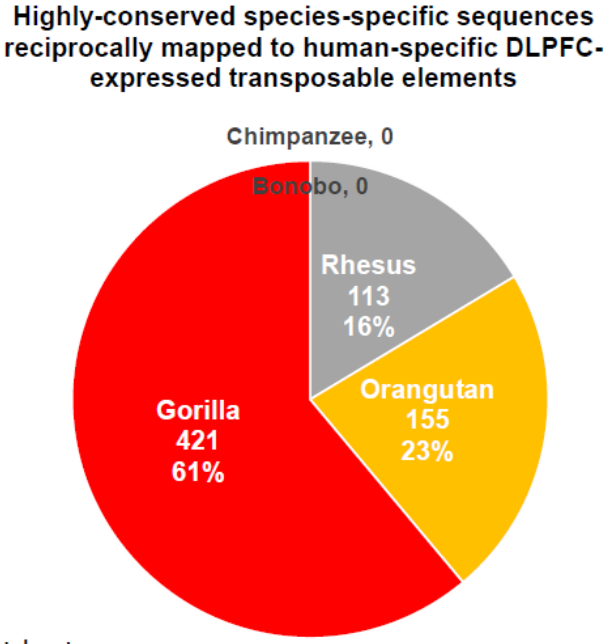

DLPFC, dorsolateral prefrontal cortex